Urban flood and waterlogging disaster simulation using SCS-CN model based on land use change in the Karst region of North China: A case of Jinan city

Shunli Hu, Fangge Zhang and Shanzhong Qi*
College of Geography and Environment, Shandong Normal University, Jinan 250358, CHINA
*shzhqi@sdnu.edu.cn

Abstract
Studying flood and waterlogging disaster risk induced by land use change would have implicational significance to urban planning and sustainability. Like other Karst landscape region, Jinan city has been also suffering from the threat of flood and waterlogging disaster, which is located in the Karst region of North China. In this study, we analyze the spatial and temporal land use change in Jinan city during 2000—2020 based on RS, GIS and field investigation. Further, using the SCS-CN model and GIS, we simulate flood and waterlogging disaster based on land use change. This study extends beyond merely furnishing scientific data support for local governmental efforts in disaster prevention and mitigation to urban flood and waterlogging.

Human encroachment on Karst mountainous areas makes these urban communities more vulnerable to flood and waterlogging hazards. Also, the urban and Karst ecosystems are fragile ecosystems, whose integration and overlap will bring about the double vulnerability for the urban ecosystem. All these could raise higher management requirements for the sustainable development of Karst urban mountainous regions in North China. In future, strengthening more protection in Karst mountainous regions of North China will become the top concern of various local governments.

Keywords: Urban flood and waterlogging, Urbanization, Land use change, SCS-CN model, Karst region of North China.

Introduction

Under the background of global climate change and rapid urbanization, extreme rainstorm events in the world have been increasing[8,15], thereby influencing hydrological cycle and increasing the possibility for flood disasters. Further, flood and waterlogging disaster have occurred more frequently within the cities over the last decades. Moreover, urban flood and waterlogging disaster are caused by extreme or continuous rainfall, thereby overwhelming the low-lying areas of cities and causing significant economic losses within the city, which is becoming more and more serious in China's modern cities[49].

**** Author for Correspondence***

For instance, the extreme rainstorm, which has occurred in Zhengzhou city of China on July 20, 2021, has resulted in 292 deaths and direct economic losses of 120.06 billion yuan[4]. Moreover, the development of urban economy has been seriously affected by urban flood and waterlogging disaster.

The life and property safety of residents within the city have been endangered. Therefore, urban flood and waterlogging disaster have become one of the major risks for the medium-to-long term urban sustainable development[10,18], especially in the Karst mountainous regions, among which surface Karst has been impacted by heavily urbanization[6].

Notably, China is a mountainous country which has been most severely affected by flood and waterlogging disasters. China's Karst mountainous geological area is about 344×10^4 km^2, which accounts for 25% of the world's carbonate rock covering about 15% of the land area on the Earth[14]. These Karst mountainous geological regions in China could be divided into the Karst Regions of South China and North China[20]. The main Karst region in North China includes Hebei, Shandong, Henan and Shanxi provinces as well as Beijing, Tianjin, Jinan, Xuzhou and Yangquan cities[9]. With the rapid urbanization development, land use change has occurred in many cities over the last decades, thereby resulting in more and more serious urban flood and waterlogging disaster, especially in most Karst region of North China.

On the other hand, the rapid development of cities is another important factor for hydrological cycle. Urban expansion will lead to change of land use type within the city, in which a large number of agricultural and forest lands turn into construction land. The spatial pattern of land use within city, which is profoundly changed by rapid urbanization, has affected the urban hydrological processes caused by the increase of impervious area of cities and increased serious urban flood and waterlogging disasters[2,16,21]. These have led to the common diseases called "every rainy day will flood" and "city looking at the sea" in most cities[28], especially in the fragile Karst mountainous regions. For example, Jinan city, one of cities belonging to the Karst region of North China, was hit by a torrential rain on July 18, 2007, which caused widespread flooding in the urban area and affected 333,000 people, with a direct economic loss of 1.23 billion yuan[43].

In addition, on July 21, 2012, an extreme rainstorm struck the Fangshan district of Beijing city (another city located in

the Karst region of North China), which caused disaster area of 16,000 km^2, the victims of probably 1,900,000 and the death toll of 79, with the economic losses of 11.64 billion yuan[45]. Moreover, with the rapid development of urbanization and civilization in the Karst mountainous regions of North China in recent years, these regions have been become urban areas, in which the Karst environments and resources are increasingly disturbed due to climate change and a large degree of the social-economic development and economic factors, thereby resulting in the changes of Karst environment and landscape in the urban mountainous regions of North China.

Further, rapid urbanization occurs and the city expands fast in a radiation manner in the Karst mountainous region of North China, thereby resulting in remarkable contradictions between population and land use. Moreover, large-scale human activities have significantly changed the natural conditions of surface Karst and aggravated the problems of regional environmental hazards[27,29,43,48].

On the other hand, the formation of flood and waterlogging disaster is related to land use, meteorology and hydrology, among which land use change is the most important factor affecting flood and waterlogging disasters[13]. Although many scholars have devoted to the study of urban flood disaster from all aspects at home and abroad, the research on flood and waterlogging disasters induced by land use change is relatively few in China. Moreover, the study area is mostly concentrated in the regions of South China where the rainfall is high. But the study area in North China is also mainly concentrated in Beijing, Zhengzhou etc. Less research on flood and waterlogging disasters has been done in the Karst region of North China.

On the other hand, many studies have been conducted in the Karst mountainous region of South China[11,12,35], but studies on urban flood and waterlogging hazards induced by land use change in the Karst mountainous region of North China are scarce. Jinan city is located in the Karst mountainous region of North China, well known for its fractured-Karst springs as well as composed predominantly of low mountains and hills.

In recent years, Jinan city have been undergoing rapid urbanization, especially in its Karst mountainous area, thereby resulting in landscape change of urban hills[43], environmental hazards within the city[29]. Also, it is suffering from the threat of flood and waterlogging disaster. Therefore, it is highly required to fill the gap by revealing the spatial and temporal change of land use in Jinan city, further simulating urban flood and waterlogging disaster using the application of SCS-CN model for the sustainable development of urban Karst mountainous region in North China.

Material and Methods

Study area: Jinan city (between 116°49′–117°14′ E and 36°32′–36°51′ N), is located in the Karst mountainous region of North China and is known as “City of Springs”. It has a typical warm-temperate, semi-humid, continental monsoon climate and well-defined seasons. The mean annual temperature is 14 °C and the average mean precipitation is 650–700 mm. City’s southern part is the Karst mountainous area, locally called “Jinan Springs Field”[27]. The study was carried out in the selected 3,268 km^2 study area. Administratively, the study area consists of 6 districts, namely Li Xia, Shi Zhong, Huai Yin, Tian Qiao, Li Cheng and Chang Qing (Figure 1).

On the other hand, Jinan city is also suffering from the threat of flood and waterlogging disaster and is now one of the twenty-five key cities of China for flood control.

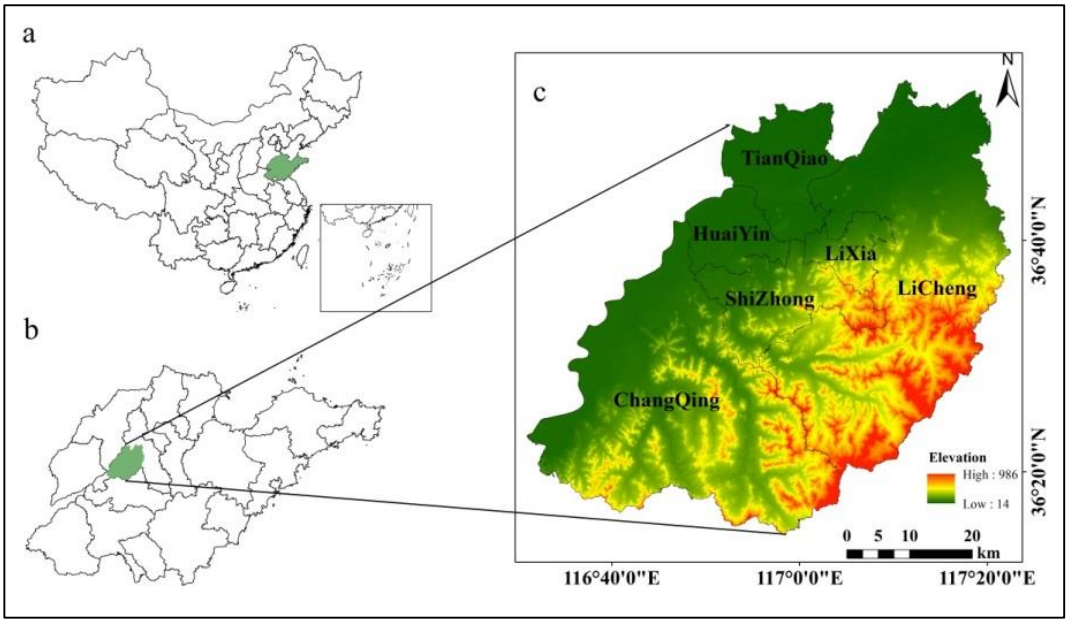

Figure 1: Details map of the study area (a China, b Shandong, c Study area)

According to the historical records, there were 110 flood and waterlogging disasters in Jinan city during the period of 1644–1911, with an average of one flood every 2.35 years[45], there were 12 floods and waterlogging disasters during the period of 1912–1948, with an average of one flood every 3.08 years[5] and there were 27 floods and waterlogging disasters during the period of 1949–2015, with an average of one flood every 2.44 years, among which three typically severe rainstorm and flood and waterlogging occurred on July 13, 1962, August 26, 1987 and July 18, 2007 respectively, thereby resulting in serious economic losses to Jinan city[44].

Data sources: The five periods of land use data from 2000 to 2020 (Landsat TM images at a resolution of 30 m taken in 2000, 2005, 2010, 2015 and 2020) were the CNLUCC (China Land Use/Land Cover Remote Sensing Monitoring) data set published by Chinese Academy of Sciences and obtained from the Resource and Environmental Science Data Platform (https://www.resdc.cn/), among which the initial projection coordinate system is krasovsky_1940_Albers and the geographic coordinate system is GCS_Krasovsky_1940. In addition, the land use data were classified into six land use types: farmland, forestland, grassland, water, built up land and unused land (https://www.resdc.cn/).

To assess land use change during the period of 2000–2020 in the study area, first, we used ArcGIS10.8 to open the land use data and cut it according to the shape of the study area; second, we use the "Projection grid" to unify the land use data into WGS_1984_UTM_Zone_50N and GCS_WGS_1984 and then we reclassified the 5-period land use data into six types applicable to the study area, namely farmland, forestland, grassland, water, built up land and unused land (Figure 2).

We collected the required other data for this study including the digital elevation model (DEM) data (with a spatial resolution of 12.5m×12.5m) obtained from the free available database of NASA (ASF Data Search (alaska.edu)), the required vector data (Shandong province boundary, Jinan city boundary and Jinan county boundary) obtained from the Public Service Platform of Geographical Information in Shandong province (https://www.sdmap.gov.cn/index.html), the soil data obtained from China Soil Database (http://vdb3.soil.csdb.cn/) (with a spatial resolution of 30m×30m) and HWSD (https://www.fao.org/) (with a spatial resolution of 1km×1km), the soil texture data obtained from the Resource and Environmental Science Data Platform (https://www.resdc.cn/) (with a spatial resolution of 1km×1km), the NDVI (2020) data obtained from the National Ecological Science Data Center (https://www.nesdc.org.cn/) (with a spatial resolution of 30m×30m).

On the other hand, we used ArcGIS10.8 to open the DEM data, soil data as well as NDVI data and combined the vector data of study area to use "Mask" tool to mask, then resampled to 30m×30m. Next, we opened the vector data of study area and got the digital soil type map of study area (Figure 3a).

Application of the SCS-CN model: The Soil Conservation Service Curve Number (SCS-CN) model has been widely used for water resource management, urban rainstorm simulation and runoff estimation[19,38,42], which was developed by the USDA-Soil Conservation Service in 1972[36].

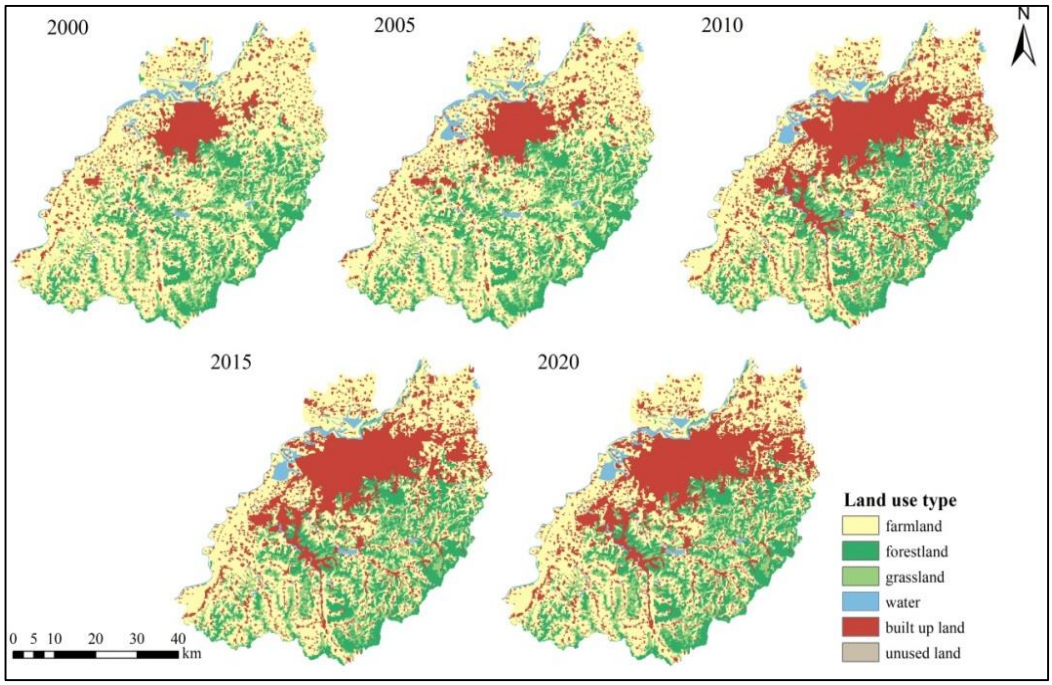

Figure 2: Classification and dynamic change of land use in the study area

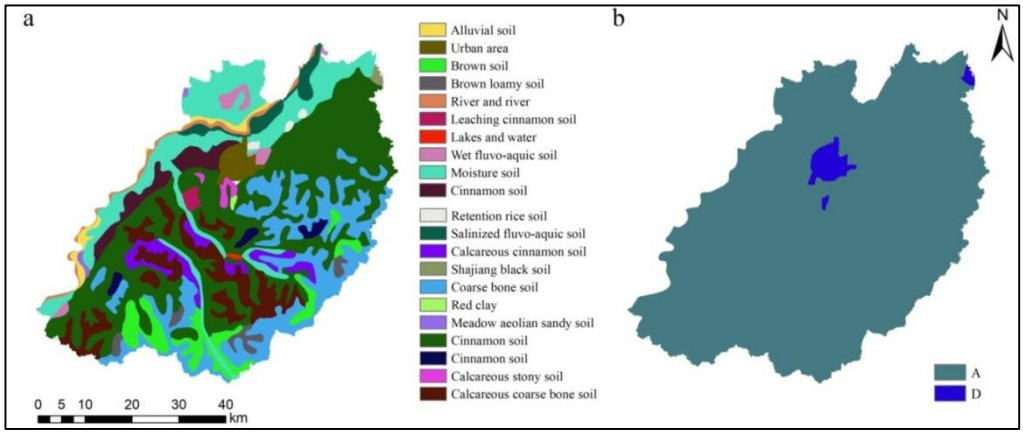

Figure 3: Distribution of soil types and hydrological soil groups in the study area (a soil types, b hydrological soil groups)

The model is based on the water balance equation and two basic hypotheses. The water balance equation is that the rainfall is equal to the amount of the initial loss, the subsequent loss and the actual surface runoff as in eq. 1. The first hypothesis is that the ratio of surface runoff to potential maximum runoff is equal to the ratio of surface infiltration to potential maximum infiltration (eq. 2). The second hypothesis is that there is a linear relationship between initial loss and potential maximum infiltration (eq. 3).

Water balance equation: $P = I_a + F + Q$ (1)

First hypothesis: $\frac{Q}{P-I_a} = \frac{F}{S}$ (2)

Second hypothesis: $I_a = \lambda S$ (3)

According to the above equations (1-3), the quantitative relationship between surface runoff and precipitation can be obtained, which can be expressed by the following equation[22,38,47]:

$$Q = \begin{cases} \frac{(P-I_a)^2}{P-I_a+S}, & P \geq I_a \\ 0, & P < I_a \end{cases} \quad (4)$$

where Q is the direct runoff (mm), P is the total precipitation (mm), I_a is the initial abstraction (mm), S is the potential maximum retention (mm), F is soil infiltration (mm) and λ is the initial abstraction coefficient. Based on the previous studies[31,32,38,42], when $\lambda = 0.2$, the standard SCS-CN model is obtained (eq. 5). Moreover, the parameter S can be represented by CN and the relationship between CN and S is expressed as in eq. 6.

$$Q = \begin{cases} \frac{(P-0.2S)^2}{P+0.8S}, & P \geq 0.2S \\ 0, & P < 0.2S \end{cases} \quad (5)$$

$$S = \frac{25400}{CN} - 245 \quad (6)$$

where CN is a dimensionless parameter, varying from 0 to 100 and also a comprehensive parameter reflecting the characteristics of the studied region before rainfall; S (mm) depends on Antecedent Moisture Condition (AMC), land use type, soil type and surface condition[23]. The CN value is determined from land use type and management and from the hydrologic soil group using a table from the SCS handbook[36]. Three AMCs are defined as drought (AMCI), normal (AMCII) and moisture (AMCIII)[19,23].

Hydrologic soil groups (HSG) is defined as the division of soils into different soil groups by American soil scientists based on the observed rainfall, runoff, soil texture and infiltration data[24,41] The HSG are divided into four types based on the different saturated hydraulic conductivity and soil texture namely A, B, C and D (Table 1). Based on the China 1:100,000 soil type map, 1:100,000 soil texture map and world soil database (HWSD) as well as the soil type map (Figure 3a), the soil types were reclassified and the hydrologic soil types in the study area were mainly A and D types (Figure 3b) according to the HSG classification standard. Due to the relative stability of soil properties in the study area during the study period, the same soil type and the same soil hydrological grouping were used.

On the other hand, the CN value is an important parameter of SCS model and reflects the runoff potential of the underlying surface. According to the CN value table proposed in chapter 9 of the National Engineering Manual of the United States[37], the CN value in the normal state (AMCII) is obtained through referring to a large number of CN value matrices used in domestic research[3,22] and combining the results of land use types and soil hydrological grouping in the study area (Table 2, Figure 4).

Referring to the tables 1 and 2, we set the CN value of AMC II (normal) for the extracted land use data, then rasterize by ArcGIS10.8. Further select the 2h cumulative precipitation of 147.95 mm during the 100-year recurrence period as the unified precipitation input in the study area and finally calculate the spatiotemporal distribution of surface runoff (runoff depth, surface runoff depth, average runoff depth and total surface runoff) and submerged water depth based on land use data in different years according to the equations (5) and (6).

Table 1
Hydrological soil types

HSG	Minimum infiltration rate (mm/h)	Soil texture
A	7.26–11.43	Sandy soil, Loam sandy soil, Sandy loam
B	3.81–7.26	Loam, Silty loam
C	1.27–3.81	Sandy sticky loam
D	0–1.27	Sticky loam, Silty sticky loam, Sandy clay, Silty clay, Clay

Table 2
CN value of AMCII state in the study area

Land use type	Classification of hydrologic soils for CN	
	A	D
Farmland	67	89
Forestland	36	79
Grassland	30	78
Water	98	98
Built up land	77	92
Unused land	72	90

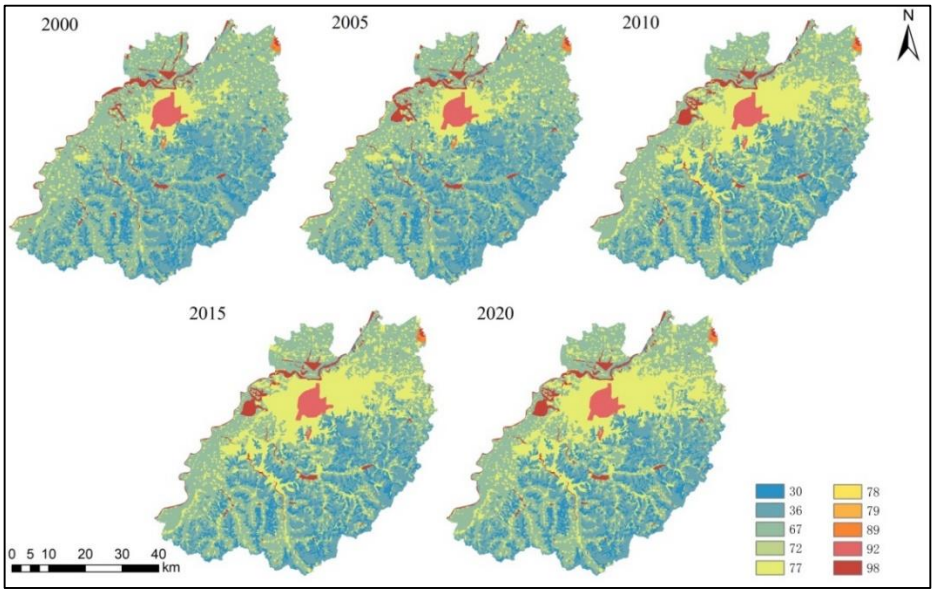

Figure 4: Distribution of CN value in the study area from 2000 to 2020

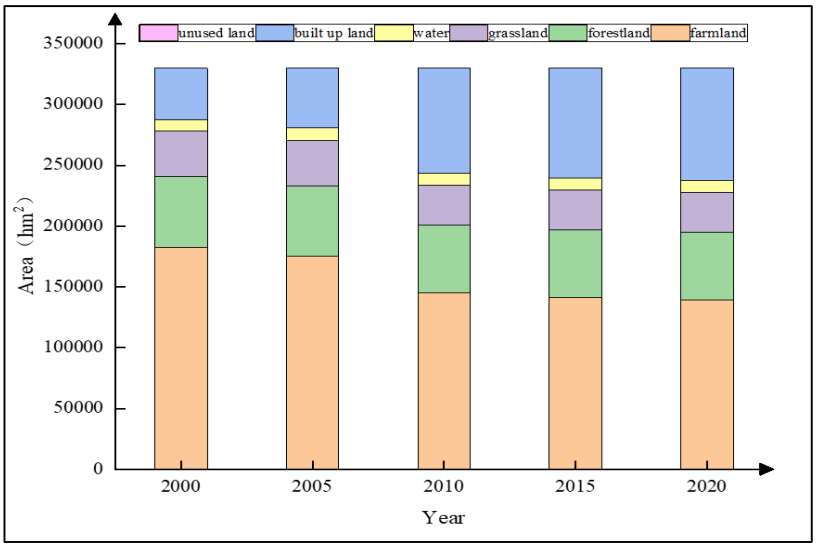

Figure 5: Area change of land use types from 2000 to 2020

Results and discussion

Land use change: The land use types in the study area were farmland, forestland, grassland, water, built up land and unused land (Figure 2). During the period of 2000—2020, farmland was the most important land use type in the study area and built up land was the second largest land use type, followed by forestland and grassland, but water area and unused land accounted for less (Figure 5). The area of built up land changed the most, which increased by 49768.02 hm^2 in 20 years, but the area of farmland decreased the most, which decreased by 43071.03 hm^2. In addition, the water area increased by 777.24 hm^2 and the area of forestland, grassland and unused land decreased by 2624.94 hm^2, 4516.83 hm^2 and 330.21 hm^2 respectively (Figure 5).

On the other hand, the spatial pattern of land use degree in the study area was obviously different and the land use intensity in the northern region was higher than that in the southern region (Figure 6). In terms of time scale, the comprehensive index of land use degree increased continuously during the period of 2000—2020, from 280.80 in 2000 to 298.01 in 2020. Moreover, the change quantity and rate of land use degree increased first and then decreased and they were positive in every period.

Effect of land use change on surface runoff: As shown in figure 7, in terms of space scale, the high value of surface runoff depth mainly appeared in the northern part of the study area and the low value mainly distributed in the southern part. The reason for this was related to the type of land use. The northern region was mainly built up land and farmland in the study area, with large impervious area, small infiltration rate and large surface runoff, but the southeastern region was the southern Karst mountainous area of Jinan city, where forestland and grassland were the main types of land use (Figure 2). Under the same rainfall scenario, the infiltration rate was higher and the surface runoff was less.

On the other hand, in terms of time scale, the concentration interval of surface runoff depth was also different under the condition of land use in different periods. On the whole, the surface runoff depth from 2000 to 2020 mainly concentrated in the interval of 32—102 mm (Figure 7). The area of this interval respectively accounted for 83.95%, 83.51%, 85.19%, 85.12% and 85.07% of the study area in each year during the period of 2000—2020, but the area difference was not big.

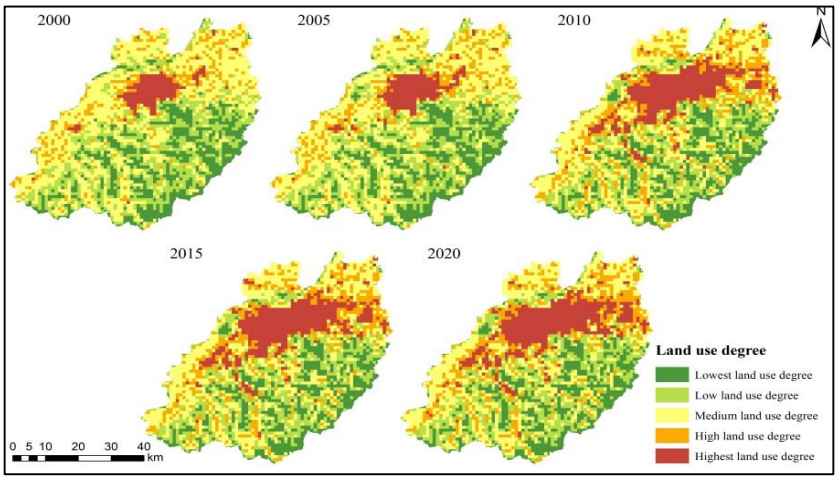

Figure 6: Spatial distribution of land use degree from 2000 to 2020

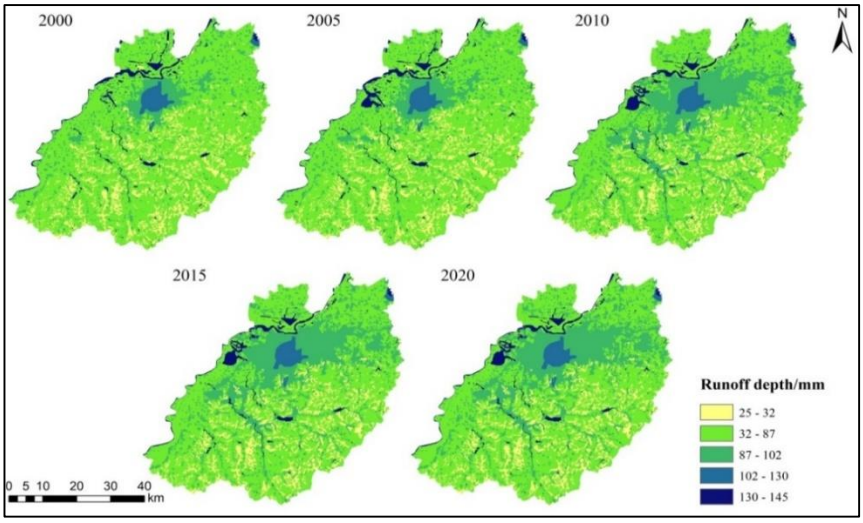

Figure 7: Distribution of runoff depth in 100-year return period

However, in 2000 and 2005, the depth of surface runoff was concentrated in the range of 32—87mm and the area proportion was 72.67% and 70.35% respectively. This was because the degree of urbanization in these two periods was low and farmland was the main type of land use in the study area (Figure 7, Figure 2). Although the surface runoff depth was still concentrated in the 32—87 mm range, the area of the 87—102 mm range could be seen to increase significantly during the period of 2010—2020 (Figure 7) and the area proportion of 87—102 mm interval was 24.59%, 25.68% and 26.20% respectively. In addition, the surface runoff depth resulted from different land use types from large to small was separately water area, built up land, unused land, farmland, forestland and grassland and this was determined by the soil infiltration rate.

Generally speaking, the higher is the vegetation coverage, the higher is the soil infiltration rate and the surface runoff from different land use types was farmland, built up land, forestland, water area, grassland and unused land. The reason was that the area of farmland in the study area was always the largest (Figure 2), so the surface runoff was the most; however, because the infiltration rate of built up land was low, so the surface runoff was second.

Further, the surface runoff change for the 100-year rainfall recurrence periods, namely, 2000—2005, 2005—2010, 2010—2015, 2015—2020 and 2000—2020, was calculated using the grid calculator respectively and the mean runoff depth and total surface runoff of each year under the case of once-in-100-year rainfall were also calculated by the modified SCS-CN model and the calculation method of mean runoff depth (Figure 8, Table 3). As shown in fig. 8, the change of surface runoff depth was mainly concentrated in the range of -100 mm—100 mm in the study area and the change of surface runoff depth caused by land use change in different periods also had obvious spatial and temporal difference.

In terms of time scale, the total amount and average depth of surface runoff increased with time. Under the scenario of once-in-100-year rainfall, the average runoff depth from 2000 to 2020 was 69.45 mm, 70.18 mm, 73.05 mm, 73.31 mm and 73.46 mm respectively and the average runoff depth during the periods of 2000—2005, 2005—2010, 2010—2015 and 2015—2020 respectively increased by 0.73 mm, 2.87 mm, 0.26 mm and 0.15 mm (Table 3). The reason was that other types of land use turned into a large number of built up land owing to the rapid urbanization development in the study area, which increased the impervious area and led to the change of runoff depth. At the same time, the increasing runoff speed increased first and then decreased, which indicated that land use change was one of the important factors affecting the change of runoff depth.

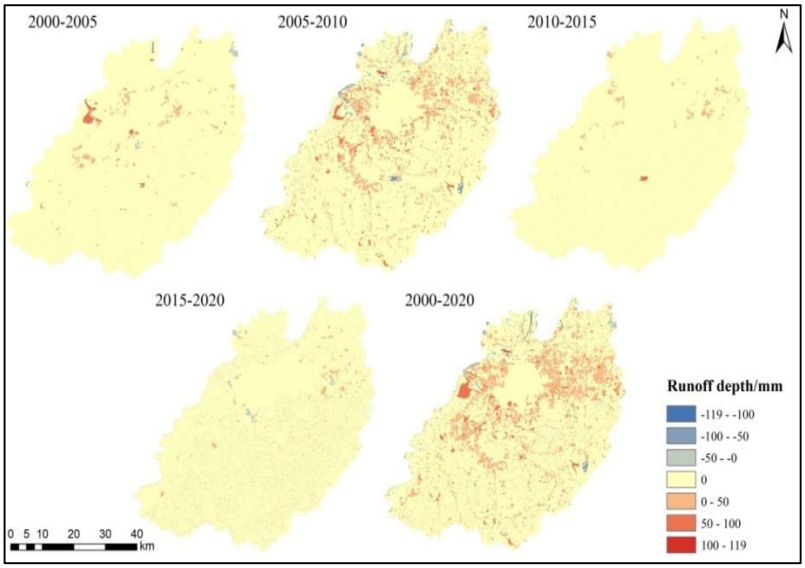

Figure 8: Variation of surface runoff depth in different periods in the study area

Table 3
Average runoff depth and total surface runoff in the study area from 2000 to 2020

Year	Average runoff depth (mm)	Total surface runoff (m^3)
2000年	69.45	229021884.1
2005年	70.18	231442597.8
2010年	73.05	240907668.1
2015年	73.31	241769177.4
2020年	73.46	242242628.4

On the other hand, from the spatial perspective, the surface runoff depth in the study area changed obviously during the whole study period from 2000 to 2020, showing a trend of "increasing around the urban area, increasing more in the East and North and increasing less in the West and South" (Figure 8), which was in line with Jinan's urban spatial development pattern of "expanding eastward, westward, south-controlled, north-spanning and middle-excellent".

Moreover, the increased depth of surface runoff (0—119 mm) was mainly distributed around the urban area, with an area of 1872.66 hm^2, accounting for 18.76% of the total area of the study area and the increase of surface runoff depth in the four periods of 2000—2005, 2005—2010, 2010—2015 and 2015—2020 accounted for 2.71%, 13.71%, 1.54% and 3.37% of the study area respectively (Figure 8). Of these, the increase in runoff in 2005—2010 was more widespread than in the three periods of 2000—2005, 2010—2015 and 2015—2020, indicating that urbanization developed fastest, urban area expanded rapidly and runoff increased to form a pattern of urban area as the center to spread around from 2005 to 2010.

Effect of land use change on submergence depth: As shown in figure 9, the submergence depth increased with time, but the overall change was not obvious and the maximum submergence depth in 2000, 2005, 2010, 2015 and 2020 was 14.867 m, 14.882 m, 14.939 m, 14.944 m and 14.947 m respectively. Moreover, the concentration range of submergence depth in each year was also different. The submergence depth mainly concentrated in the interval of 0—1.93 m from 2000 to 2010 and the submergence depth mainly concentrated in the interval of 0.93—5.94 m from 2010 to 2020.

In addition, the total amount of surface runoff also increased with time. The total amount of surface runoff from 2000 to 2020, generated under the 100-year rainfall scenario, was 2.290×10^8 m^3, 2.314×10^8 m^3, 2.409×10^8 m^3, 2.418×10^8 m^3 and 2.422×10^8 m^3 respectively.

On the other hand, in terms of inundation extent, the inundated areas were mainly distributed in the northern part of the study area, while the high-value areas were concentrated near the low-lying of Xiaoqing river. Moreover, the submerged area gradually expanded and had the tendency of spreading in the north and scattered to the middle. With the development of Jinan city's urban planning, increasing urbanization and drastic changes in land use, the rapid expansion of built up land eroded farmland and forestland and the vegetation coverage decreased greatly, which increased runoff-producing capacity and reduced the interception capacity of runoff, thus resulting in the continuous increases of submerged depth and area.

Conclusion

The formation of flood and waterlogging disaster is related to land use, meteorology and hydrology, among which land use change is the most important factor affecting flood and waterlogging disasters especially in the fragile Karst mountainous regions of North China.

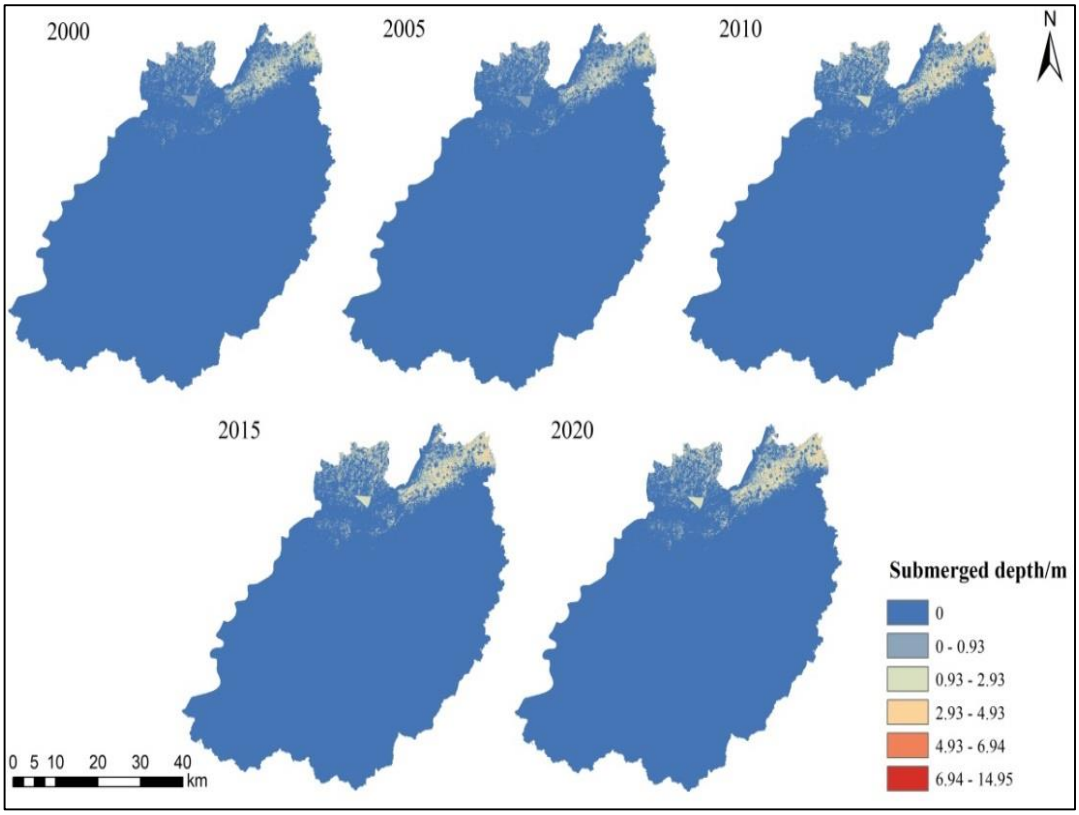

Figure 9: Distribution of submerged water depth with return period of 100 years

This study analyzed the spatial-temporal change of land use in Jinan city during 2000—2020 based on RS, GIS and field investigation and then simulated flood and waterlogging disaster based on land use change using the SCS-CN model and GIS under the scenario of once-in-100-year rainfall. The results indicate that the widespread changes of land use have taken place Jinan city of the Karst region of North China from 2000 to 2020. Built up land has increased by 49768.02 hm^2 in the study area. By comparison, cropland, forestland and grassland decreased by 43071.03 hm^2, 2624.94 hm^2 and 4516.83 hm^2 respectively. Owing to land use change induced by rapid urbanization, on the whole, the high value of surface runoff depth mainly appeared in the northern part of the study area and the low value mainly distributed in the southern part from the spatial perspective. But the surface runoff depth from 2000 to 2020 mainly concentrated in the interval of 32—102 mm in terms of time scale. Under the scenario of once-in-100-year rainfall, the change of surface runoff depth was mainly concentrated in the range of -100 mm—100 mm in the study area and the change of surface runoff depth caused by land use change in different periods also had obvious spatial and temporal difference during the period of 2000—2020.

On the other hand, surface runoff depth and surface runoff amount were different in different land use types and the surface runoff depth is water area, built up land, unused land, farmland, forestland and grassland in order from large to small, but surface runoff from large to small was farmland, built up land, forestland, water area, grassland and unused land. In addition, the submergence depth increased with time, but the overall change was not obvious. Moreover, the total amount of surface runoff also increased with time. In terms of inundation extent, the inundated areas were mainly distributed in the northern part of the study area, while the high-value areas were concentrated near the low-lying of Xiaoqing River and the submerged area gradually expanded and had the tendency of spreading in the north and scattered to the middle.

Because the urban and Karst ecosystems are fragile ecosystems, whose integration and overlap will bring about the double vulnerability of the urban ecosystem, so human encroachment on Karst mountainous areas made these urban communities more vulnerable to flood and waterlogging hazards. These could raise higher management requirements for the sustainable development of Karst urban mountainous regions in North China. In future, strengthening more protection in these regions will become the top concern of various local Governments of North China.

Acknowledgement

We acknowledge M.S. Student Qian Liu for dealing with all figures for this manuscript.

References

1. Bayrakdar C., Döker M.F. and Keserci F., An example for the disasters caused by improper land use: The Kayakoy Polje flood of January 31, 2019, *Journal of Geography-Cografya Dergisi*, **41**, 109–128 **(2020)**

2. Brath A., Montanari A. and Moretti G., Assessing the effect on flood frequency of land use change via hydrological simulation (with uncertainty), *Journal of Hydrology*, **324**, 141–153 **(2006)**

3. Chen J.M., Spatial division and feature analysis of the disaster risk of urban water logging in Fuzhou based on the SCS-CN, *Geospatial Information*, **18(4)**, 92–95 **(2020)**

4. Chen Z.Y. and Kong F., Study on fragmentation of emergency management during "7·20" extreme rainstorm flood disaster in Zhengzhou of Henan Province and relevant comprehensive treatment, *Water Resources and Hydropower Engineering*, **53(8)**, 1–14 **(2022)**

5. Committee for the compilation of historical records of Jinan, City records of Jinan, Beijing, Zhonghua Book Company Press **(1997)**

6. Ford D.C. and Williams P.W., Karst geomorphology and hydrology, London, Unwin Hyman Ltd. **(1989)**

7. Fu X.H., Analysis of land use cover change and its influences on flood vulnerability in Dongting Lake Region, Master's dissertation of Hunan Normal University **(2014)**

8. Groisman P.Y. et al, Changes in the probability of heavy precipitation: Important indicators of climatic change, *Climatic Change*, **42(1)**, 243–283 **(1999)**

9. He K.Q., Wang B. and Du R.L., Karst collapse in North China, Beijing, Geological Press **(2005)**

10. Huang G.R. et al, Study on risk analysis and zoning method of urban flood disaster, *Water Resources Protection*, **36(6)**, 1–6 **(2020)**

11. Huang M., Qi S.Z. and Shang G.D., Karst landslides hazard during 1940–2002 in the mountainous region of Guizhou Province, Southwest China, *Natural Hazards*, **60**, 781–784 **(2012)**

12. Huang Q., Cai Y. and Xing X., Rocky desertification, anti-desertification and sustainable development in the Karst mountain region of Southwest China, *Ambio*, **37**, 390–392 **(2008)**

13. Jiang Y. et al, Land use change in Zhengzhou during 2000–2021 and its impact on comprehensive runoff coefficient, *Pearl River*, **43(11)**, 98–107 **(2022)**

14. Jiang Y.J. and Yan J., Effects of land use on hydrochemistry and contamination of Karst groundwater from Nandong underground river system, China, *Water Air and Soil Pollution*, **210**, 123–141 **(2010)**

15. Kamae Y. et al, Atmospheric rivers bring more frequent and intense extreme rainfall events over East Asia under global warming, *Geophysical Research Letters*, **48**, e2021GL096030 **(2021)**

16. Khan S.D., Urban development and flooding in Houston Texas, inferences from remote sensing data using neural network technique, *Environmental Geology*, **47**, 1120–1127 **(2005)**

17. Lee Y. and Brody S.D., Examining the impact of land use on flood losses in Seoul, Korea, *Land Use Policy*, **70**, 500–509 **(2018)**

18. Li C.C., Tian J.C. and Shen R.Z., Review on assessment of flood and waterlogging risk, *Journal of Catastrophology*, **35(3)**, 131–136 **(2020)**

19. Liu X.Z. and Li J.Z., Application of SCS model in estimation of runoff from small watershed in Loess Plateau of China, *Chinese Geographical Science*, **18(3)**, 235–241 **(2008)**

20. Lu Y.R., China Karsts: landscape, types and rules, Beijing, Geological Press **(1986)**

21. Luo K. and Zhang X., Increasing urban flood risk in China over recent 40 years induced by LUCC, *Landscape & Urban Planning*, **219**, 104317 **(2022)**

22. Ma L.J. et al, Regional runoff characteristics in Zhengzhou city based on SCS-CN model, *Bulletin in Soil and Water Conservation*, **42(4)**, 203–209 **(2022)**

23. Mishra S.K. and Singh V.P., Soil conservation service curve number (SCS-CN) methodology, Kluwer Academic Publishers, Dordrecht, The Netherlands **(2003)**

24. Musgrave G.W., How much of the rain enters the soil? Water: The yearbook of agriculture, Washington D C, U.S. Gov. Print. Off. U.S., Department of Agriculture, 151–159 **(1955)**

25. Philip M., Patrick V. and Joel N., Quantitative analysis of the impacts of climate and land-cover changes on urban flood runoffs: a case of Dar es Salaam, Tanzania, *Journal of Water and Climate Change*, **12(6)**, 2835–2853 **(2021)**

26. Qi S.Z., Cao S.F., Hu S.L. and Liu Q., Bibliometric analysis on urban flood and waterlogging disasters during the period of 1998—2022, *Natural Hazards*, **120**, 12595–12612 **(2024)**

27. Qi S.Z., Guo J.M., Jia R. and Sheng W.F., Land use change induced ecological risk in the urbanized Karst region of North China: a case study of Jinan city, *Environmental Earth Sciences*, **79(12)**, 280 **(2020)**

28. Qi S.Z., Heng F.X. and Ji L.N., Landscape change of land use in the Karst region of Jinan city, North China, *Journal of Environmental Engineering and Landscape Management*, **31(1)**, 1-8 **(2023)**

29. Qi S.Z. and Zhang X.X., Urbanization induced environmental hazards from breakage hills in the Karst geological region of Jinan City, China, *Natural Hazards*, **56(3)**, 571–574 **(2011)**

30. Peng J. et al, Storm flood disaster risk assessment in urban area based on the simulation of land use scenarios: A case of Maozhou Watershed in Shenzhen City, *Acta Ecologica Sinica*, **38(11)**, 3741–3755 **(2018)**

31. Sahu R.K., Mishra S.K. and Eldho T.I., Comparative evaluation of SCS-CN-inspired models in applications to classified datasets, *Agricultural Water Management*, **97(5)**, 749–756 **(2010)**

32. Santikari V.P. and Murdoch L.C., Including effects of watershed heterogeneity in the curve number method using variable initial abstraction, *Hydrology and Earth System Sciences*, **22**, 4725–4743 **(2018)**

33. Song X.M., Zhang J.Y., He R.M., Zou X.J. and Zhang C.H., Urban flood and waterlogging and causes analysis in Beijing, *Advances in Water Sciences*, **30(2)**, 153–165 **(2019)**

34. Sun D.C., Wang H.M., Huang J. and Liu G.F., Analysis of urban flood Disaster risk in the Poyang Lake Basin and land type adjustment strategy study: A case study of Jingdezhen City, *Resources and Environment in the Yangtze Basin*, **27(12)**, 2856–2866 **(2018)**

35. Tong X.W. et al, Increased vegetation growth and carbon stock in China Karst via ecological engineering, *Nature Sustainability*, **1**, 44–50 **(2018)**

36. USDA SCS, National Engineering Handbook, Section 4, Hydrology, USDA-SCS, Washington, D.C. **(1985)**

37. USDA NRCS, National Engineering Handbook, Title 210-VI, Part 630, Chapter 9, Hydrologic Soil-Cover Complexes. Washington DC, U.S. Department of Agriculture, Natural Resources Conservation Service **(2004)**

38. Verma S. et al, Activation soil moisture accounting (ASMA) for runoff estimation using soil conservation service curve number (SCS-CN) method, *Journal of Hydrology*, **589,** 125114 **(2020)**

39. Wan R.R. and Yang G.S., Discussion on some issues of hydrological effects of watershed land use and land cover change, *Progress in Geography*, **24(3)**, 25–33 **(2005)**

40. Wang Y.L. and Yang X.L., Land use/cover change effects on floods with different return periods: a case study of Beijing, China, *Frontiers of Environmental Science & Engineering*, **7(5)**, 769–776 **(2013)**

41. Woodward D.E., Hawkins R.H. and Quan Q.D., Curve number method: origins, applications and limitations. Hydrologic modeling for the 21st century. Second federal interagency hydrologic modeling conference, July 28 to August 1, Las Vegas, Nevada **(2002)**

42. Xiao B. et al, Application of the SCS-CN model to runoff estimation in a small watershed with high spatial heterogeneity, *Pedosphere*, **21(6)**, 738–749 **(2011)**

43. Xu Y.T., Qi S.Z., Wang G.W. and Shang G.D., Urbanization induced landscape change of urban hills in Jinan City, Karst geological region of North China, *Landscape Research*, **37(6)**, 721–726 **(2012)**

44. Zhang S., Guo J., Gao Z. and Jiang Y., The 2007 urban flood in the Jinan City, *Yellow River*, **32(2)**, 30–31 **(2010)**

45. Zhang X. and Zhao J.B., Study on flood disasters in the Qing dynasty in Jinan city, *Journal of Shaanxi Normal University (Natural Scientific Edition)*, **37(4)**, 95–100 **(2009)**

46. Zhang X.X., Sheng W.F. and Qi S.Z., Hazards and reflection on Fangshan District extreme rainstorm of July 21, 2012, the urban mountainous region of Beijing, North China, *Natural Hazards*, **94(3)**, 1459–1461 **(2018)**

47. Zhao W.C. et al, Ridge surface runoff estimation for micro-

rainwater-harvesting-ridges on slopping land in the hilly areas of the Loess Plateau based on SCS-CN model, *Chinese Journal of Ecology*, **41(1)**, 199–208 **(2022)**

48. Zheng Z.P. and Qi S.Z., Potential flood hazard due to urban expansion in the Karst mountainous region of North China, *Regional Environmental Change*, **11(3)**, 439–440 **(2011)**

49. Zheng Z.P., Qi S.Z. and Xu Y.T., Questionable frequent occurrence of urban flood hazards in modern cities of China, *Natural Hazards*, **65,** 1009–1010 **(2013)**.

(Received 01st January 2025, accepted 05th March 2025)